Comparison between Sentinel-2 and WorldView-3 sensors in mapping wetland vegetation communities of the Grassland Biome of South Africa, for monitoring under climate change

H. van Deventer [a,b,*], A. Linström [c], L. Naidoo [d], N. Job [e], E.J.J. Sieben [f], M.A. Cho [a,g,h]

[a]Council for Scientific and Industrial Research, Pretoria, South Africa
[b]Department of Geography, GeoInformatics & Meteorology Geography, University of Pretoria, Pretoria, 0083, South Africa
[c]Wet Earth Eco Specs (Pty) Ltd, P.O. Box 4442, 58 Kerk St, Lydenburg, 1120, South Africa
[d]Gauteng City-Region Observatory (GCRO), a Partnership of the University of Johannesburg, the University of the Witwatersrand, Johannesburg, the Gauteng Provincial Government and Organised Local Government in Gauteng (SALGA), 11 Jorissen St, Braamfontein, Private Bag 3, Johannesburg 2050, South Africa
[e]Freshwater Biodiversity Unit, South African National Biodiversity Institute (SANBI), South Africa
[f]School of Agricultural, Earth and Environmental Sciences, University of KwaZulu-Natal, Private Bag X54001, Westville, 4001, South Africa
[g]School of Agriculture, Earth and Environmental Sciences, University of KwaZulu-Natal (UKZN), Private Bag X01, Carbis Road, Scottsville, Pietermaritzburg, 3201, Bag X01, South Africa
[h]Plant and Soil Sciences, University of Pretoria, Private Bag X20, Hatfield, 0028, South Africa

* Corresponding author. Council for Scientific and Industrial Research, Pretoria/Stellenbosch, South Africa.
Email: HvDeventer@csir.co.za

Highlights

- Palustrine wetlands are highly separable from terrestrial grasslands (>91%). This means that changes in the areal extent of palustrine wetlands can be reported in the next cycle; for the Sustainable Development Goal (SDG) to sub-indicator 6.6.1a.
- Several wetland vegetation communities could be mapped, suggesting improved biodiversity reporting to SDG 15 and monitoring for threatened species.
- The red-edge and shortwave infrared bands played an important role in improved separability of vegetation classes in these study areas. This study tested the contribution of the Sentinel-2 SWIR bands in vegetation mapping which has not been explored for this particular sensor.

Abstract

Monitoring changes in the areal extent and geographic distribution of wetland vegetation has become more critical considering the impact of anthropogenic and climate changes. We compared the capabilities of the optical space-borne sensors Sentinel-2 and WorldView-3 (WV3) to distinguish between wetland and terrestrial vegetation for improved reporting to the Sustainable Development Goal (SDG) sub-indicator 6.6.1a, and also map different wetland vegetation communities for two catchments in the Grassland Biome of South Africa. Ground truthing of vegetation communities was conducted between 2016 and 2018. A Random Forest classification algorithm was used with a 100-fold cross-validation to assess mean accuracies using all combinations of bands, a digital elevation model generated from fine-scale contours, spectral vegetation indices (VIs) and above-ground biomass (AGB). Five and eight wetland vegetation classes were mapped for Hogsback and Tevredenpan, respectively, of a total of 13 classes for each of the sites. Wetland and terrestrial vegetation were found to be highly separable, with overall accuracies (OAs) attaining 91–99% and

individual user's accuracies 88–99% for both sensors and study areas. Even though the wetland vegetation communities consisted of a mosaic of smaller communities, monodominant species and plant functional type classes, they were found to be highly separable across sensors and study areas. The highest average OA of 83% for Hogsback's wetland vegetation communities was achieved using WV3 bands with elevation, AGB and the VIs, while the Sentinel-2 bands, elevation, AGB and VIs attained an average OA of 78%. For Tevredenpan, the use of the Sentinel-2 bands and elevation achieved the highest mean OA of 79% for the classification of wetland vegetation communities, while the WV3 (in this case the short-wave infrared bands were not available owing to shortage of funding) maximized at 74%. The inclusion of elevation data and spectral indices in the classification scenarios of wetland vegetation communities increased the OA by 4–17%. Omitting the red-edge and shortwave infrared bands for classification of vegetation classes resulted in a varied response across sensors and study areas, but decreased the OA by 4.8–7.3% when using the Sentinel-2 sensors. These results show promise for improved reporting and monitoring of the extent and types of palustrine wetlands in the Grassland Biome of South Africa using freely-available Sentinel-2 data.

Keywords: Freshwater ecosystems; Palustrine wetlands; Random forest; Sustainable development goals (SDGs) 6 and 15

1. Introduction

Monitoring changes in the areal extents and geographic distribution of wetlands, a highly threatened realm, are critical to tracking changes in their biodiversity and ecosystems (IPBES, 2019). In 2020, the first changes in the extent of wetlands were reported to the United Nations as part of SDG 6.6, which stated: 'By (2020), protect and restore water-related ecosystems, including mountains, forests, wetlands, rivers, aquifers and lakes' (UN, 2017). For the sub-indicator 6.6.1a, the areal extent of lacustrine (open water) and palustrine (vegetated) wetlands was reported (UN, 2017). These are the two biomes identified under the wetland realm in the latest global ecosystem types (Keith et al., 2020), serving as coarse-scale surrogates of wetland biodiversity. Only lacustrine biome wetlands were reported to the UN by 2020 as part of SDG 6.6.1a, and many countries depended on the Global Surface Water products, derived from 30-m spatial resolution Landsat series and Sentinel-2 images (Pekel et al., 2016). Information on changes in the areal extent of palustrine wetlands was lacking globally. At the same time, comparison with wetlands on a country-wide scale also showed an extensive underrepresentation of lacustrine wetlands (Van Deventer, 2021), and very likely a global trend, though evidence lacking elsewhere.

The impact of global changes on the areal extent and geographic distribution of palustrine wetlands remains a knowledge gap. Changes in the extent, composition, physiology, and phenology of plant species, resulting from anthropogenic and climate changes, have been observed since the 1970s (Campoy et al., 2011; Sardans and Peñuelas, 2012; Richardson et al., 2013). Fewer studies have assessed the separability of wetland from terrestrial vegetation for SDG 6.6.1a reporting, or mapping of the areal extent and geographic distribution of wetland vegetation communities, particularly in the Grassland Biomes where vegetation height does not always differ across a wetland-terrestrial gradient. This biome covers approximately 40% of the earth's surface area (excluding the Greenland and

Antarctica continents), showing high degrees of land conversion to agriculture and urban areas and/or degradation (WRI, 2000). In South Africa, the Grassland Biome constitutes 26% of the extent of South Africa's land surface and shows the second-highest rate of loss of all biomes in the country (Skowno et al., 2019). The impacts of climate change are expected to shift the aridity gradient in South Africa further eastwards towards the Highveld Region (Mofutsanyana, 2017; Mofutsanyana et al., 2020), while bush encroachment from the Savannah Biome into the grasslands is also a concern (Bond and Midgley, 2012; Stevens et al., 2016). The invasion of robust clonal species, including indigenous *Phragmites australis* and *Typha capensis* or invasives, is expected to invade vulnerable wetland types, for example, those dominated by sedges (Mulhouse et al., 2005) with a decline in rhizomatous graminoids (Mofutsanyana, 2017; Mofutsanyana et al., 2020). Therefore, the detection and monitoring of changes in the extent and climatic ranges of species are critical. Remote sensing can supplement point-based assessments should vegetation communities be spectrally separable.

Several studies have evaluated the separability of wetland vegetation types or communities in the Grassland Biome at landscape level using optical, space-borne multispectral images (Drovnova et al., 2012; Bochenek et al., 2013; Dubeau et al., 2017; Rapinel et al., 2019; Bhatnagar et al., 2020) and at finer scales using methods such as unmanned aerial vehicles (UAVs) (Knoth et al., 2013; Beyer et al., 2019). Accuracies reported for these studies ranged from 71 to 94% for space-borne sensors and 84–95% for the UAV studies, with both studies undertaken in palustrine wetlands with grasses and sedges and other vegetation types (Drovnova et al., 2012; Bochenek et al., 2013; Knoth et al., 2013; Crichton et al., 2015; Dubeau et al., 2017; Beyer et al., 2019; Rapinel et al., 2019; Bhatnagar et al., 2020). Several studies have assessed broad habitat types of wetland vegetation in the coastal regions of South Africa using Landsat 1, WorldView-2, RapidEye and SPOT-6 (Jarman, 1981; Lück-Vogel et al., 2016; Van Deventer et al., 2017, 2019). Overall accuracies (OAs) ranged between 64.3% and 86% and included some terrestrial classes, and palustrine wetland habitats in estuarine environments. Inclusion of ancillary data, such as elevation or indices, has been tested in other applications, with some authors reporting improvement in the predictive capabilities of remote sensing models for vegetation studies (Crichton et al., 2015; Zoungrana et al., 2015; Liu et al., 2017; Rajah et al., 2019; Niculescu et al., 2020), while other studies reported no improvement from including ancillary data (Ferreira et al., 2016). Despite these advances on detection and characterization of different palustrine wetland types, there is still a lack of reporting the extent of this biome to SDG 6. Further work is required on mapping inland palustrine wetlands, particularly for the Grassland Biome, to assess how separable these palustrine wetlands are from terrestrial vegetation, and whether the vegetation communities can be monitored and reported to SDG 6.

The availability of more recently-launched, space-borne sensors, such as Sentinel-2, WorldView and RapidEye, provides new opportunities for assessing the capabilities of these sensors to map the extent of palustrine wetlands and their plant species composition. These sensors have added bands in the red-edge and shortwave-infrared (SWIR) region of the electromagnetic spectrum (EMS), which have proved to be advantageous in separating plant species from one another in various climatic regions and habitats. Several authors have demonstrated the importance of the new bands, such as the red-edge and SWIR bands, using WorldView-2 (WV2), WV3 or RapidEye images for mapping vegetation types, with an

increase in OA of up to 14% (Immitzer et al., 2012; Pu and Landry, 2012; Omer et al., 2015; Ferreira et al., 2019; Van Deventer et al., 2019). However, the potential influence of the SWIR bands of Sentinel-2 on the classification accuracy of wetland vegetation mapping communities has not yet been assessed. Furthermore, the Sentinel-2 twin sensors, Sentinel-2A (S2A) and Sentinel-2B (S2B), launched in 2015 and 2017, respectively, by the European Space Agency (ESA), are freely available for public use, enabling regional monitoring around the world. The sensor has ten bands across the visible, near infrared (NIR), red-edge and SWIR bands at a spatial resolution of 10 and 20 m, with three additional bands at 60-m spatial resolution used for atmospheric correction (European Space Agency, 2019b). The WorldView-3 (WV3) sensor, a proprietary sensor launched on August 13, 2014 (Digital Globe Pty Ltd), provides eight multispectral bands at 1.24 m spatial resolution and eight SWIR bands at 3.7 m spatial resolution with a swath width of 13.1 km (Digital Globe Pty Ltd, 2014). WV2, for example, showed superior performance in the classification of 17 wetland vegetation species in the United States of America, outperforming traditional four-band sensors such as QuickBird, IKONOS and OrbView-3 by > 5% in OA (Carle et al., 2014). However, it remains to be assessed whether Sentinel-2 has comparable performance to WorldView sensors, since WorldView data are costly to use for monitoring, and whether the red-edge and SWIR bands of these sensors improves separability of vegetation types or communities.

The aim of this study was to compare the capability of the freely available Sentinel-2 and WorldView-3 images to map palustrine wetlands in the Grassland Biome of South Africa. The objectives of the study were:

(i) Compare the capabilities of the Sentinel-2 and WV3 optical sensors to map the areal extent of palustrine wetlands for SDG 6.6.1a reporting;

(ii) Compare the accuracies of mapping wetland vegetation communities using the Sentinel-2 and WV3;

(iii) Ascertain whether ancillary data, such as elevation models and spectral indices, would improve the classification accuracies when using Sentinel-2 and WV3 images;

(iv) Determine the contribution of the red-edge and SWIR bands to mapping vegetation communities with the Sentinel-2 and WV3 optical sensors.

Two study areas from the Grassland Biome were used to test the sensors' capabilities, near Hogsback in the Eastern Cape Province and Tevredenpan in the Mpumalanga Province. We intend for the results to inform the choices of sensors to monitor potential changes in the distribution of wetland vegetation resulting from the impacts of climate change.

2. Materials and methods

2.1. Study areas

Owing to the threat of high levels of transformation of the Grassland Biome in South Africa (Fourie et al., 2014; Skowno et al., 2019), two study areas have been chosen in this biome (Fig. 1A) for two reasons: (a) areas with palustrine wetlands were considered

underrepresented on the South African National Wetland Maps (NWMs; Van Deventer et al., 2020b); and (b) the challenge of separating sedges and grasses in palustrine wetlands from terrestrial grasses, because they can be spectrally and structurally similar. While hyperspectral and super-spectral data can very likely separate these communities (e.g., Schmidt and Skidmore, 2003; Gianinetto and Lechi, 2004), the challenge remains to assess the capabilities of freely available images from Sentinel-2.

(i) Hogsback 'Die Vlei' wetlands, Eastern Cape Province

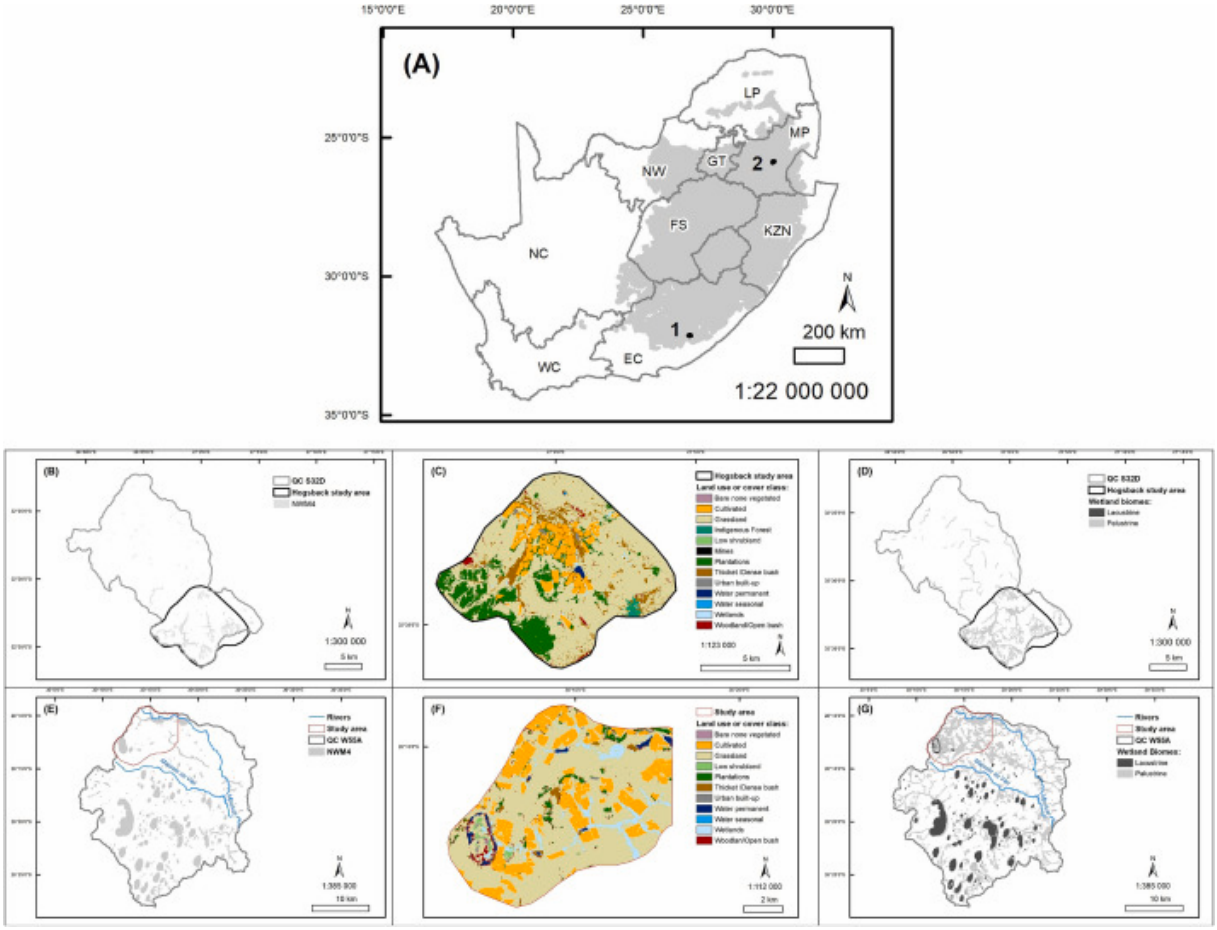

Fig. 1. Location of the study areas (A) relative to the provinces of South Africa with the two study areas being 1 = Hogsback and 2 = Tevredenpan relative to the extent of the Grassland Biome; (B) representation of wetlands in National Wetland Map version 4 (NWM4; Van Deventer et al., 2016) for the Hogsback study area, relative to those in the quaternary catchment; (C) the land cover data of 2013/4 of Hogsback (GTI, 2015); (D) the extent of wetlands in the updated NWM5 (Van Deventer et al., 2020b) for Hogsback after the output of specialist mapping (Van Deventer et al., 2020a) and relative to those of the quaternary catchment; (E) the extent of wetlands of NWM4 for Tevredenpan relative to those of the quaternary catchment; (F) land cover data of Tevredenpan; and (G) the extent of wetlands as updated in NWM5 for the Tevredenpan study area relative to those in the quaternary catchment.

The Hogsback study area (32.55°S, 26.97°E; total areal extent 8363 ha) is located north-east of the town of Hogsback in the Eastern Cape Province (Fig. 1B) in the quaternary catchment S32D (which totals 30 724 ha in areal extent). The Great Winter-Amathole Mountains is situated to the south of the study area, where vegetation consists primarily of Amathole

Montane and Mistbelt Grassland vegetation types with narrow patches of Southern Mistbelt Forests and poorly protected Eastern Temperate Freshwater Wetlands associated with the Klipplaats River (Mucina and Rutherford, 2006). The Mean Annual Precipitation (MAP) ranges from 600 to 700 mm, while the mean annual evapotranspiration is between 1600 and 1700 mm (Water Resources Atlas of 2012 [WR 2012]; Bailey and Pitman, 2016). The geology consists primarily of the Karoo Supergroup (Adelaide and Tarka subgroups), interrupted by dolerites (South African Council for Geoscience geology map 1:250 000, 3226 King William's Town, dated 1976). Wetlands occur on steep to low gradient slopes as well as the valley bottom, giving rise to the Klipplaats River. Criss-crossing dolerite dikes impede flow, resulting in constriction and backing up of the river, forming a large wetland on either side of the river in the valley. The interflow from hillslope seeps drains through valley-bottoms towards the main floodplain system, with all wetlands predominantly palustrine. The elevation of the Hogsback study area ranges from 1190 to 1960 m above mean sea level (calculated from 5-m interval contours [DRDLR:NGI, 2016]) with deep incised valleys stretching north from the mountaneous watershed division.

Approximately 2% (680 ha) of the surface area of quaternary catchment S32D (29 860 ha) was mapped in NWM4 (Van Deventer et al., 2016) as inland wetlands (Fig. 1B), although omissions were apparent from Google Earth Pro images (GEP, 2022) prior to the beginning of the project. The wetlands are largely vegetated with little open water, except for the Klipplaats River channel that flows northward. The National Land Cover layer (GTI, 2015) indicates that most of the wetlands are ‘grasslands’, while the large valley-bottom wetland on either side of the Klipplaats River is shown as ‘Thicket/Dense bush’.

(ii) Tevredenpan study area, Mpumalanga Province

The Tevredenpan study area (26.2°S, 30.2°E; ±8000 ha) is in the northern part of the Mpumalanga Lake District (MLD) of South Africa (Fig. 1C). It is located within a larger quaternary catchment W55A (with a total extent of 68 870 ha) of which 8181.8 ha of wetlands (12% of W55A's extent) were mapped in NWM4 (Van Deventer et al., 2016), hosting a large number, 416, of freshwater depressions (Van Deventer et al., 2022). In the Tevredenpan study area, 952.8 ha of wetlands (also 12% of the extent of the study area) were mapped in NWM4. The vegetation type in the catchment is described as the ‘Eastern Highveld Grassland Biome’ and is considered ‘hardly protected’ (Mucina and Rutherford, 2006). The Tevredenpan study area is in the western section of the sub-quaternary catchment SQ4#1375, mapped as predominantly grassland, and hosting large valley-bottom systems, seeps, and some depressions. The largest of the depressions within the study area is Tevredenpan (Fig. 1). The area receives between 600 and 700 mm of MAP, while the mean annual evapotranspiration range is between 1700 and 1800 mm per annum (WR 2012; Bailey and Pitman, 2016).

The elevation of the study area ranges from 1700 to 1820 m above mean sea level (calculated from 5-m interval contours [DRDLR:NGI, 2016]), reflecting gradually undulating slopes of the plateau, with valleys draining to the east. The geology in the study area is primarily Vryheid formation (Pv), where the coal mining takes place with intermittent dolerites (Jd) to the east and surface alluvium deposits (Q) (Council for Geoscience

Table 1. Image acquisition dates for the Sentinel-2 and WorldView-3 (WV3) sensors for the Hogsback and Tevredenpan study areas. GMT - Greenwich Meridian Time, MIR = mid-infrared region of the EMS, SWIR - shortwave infrared, VIS = visible range of the electromagnetic spectrum (EMS).

Sensor	Sentinel-2A	WV3
Hogsback	2016/12/03 at 07:53 GMT, 13 bands	Multispectral data for two dates: •2016/10/18 VIS-MIR •2016/12/25 VIS, MIR, and SWIR taken at 8h41 Greenwich Mean Time (GMT)
Tevredenpan	2017/01/19 at 07:42 GMT, 13 bands	2017/03/21 at 08:27:09 GMT including VIS-MIR

1:250 000 geology map 2630 Mbabane printed in 1986). The Vryheid formation is relatively flat, with slow mudstone eroding into depressional systems (McCarthy et al., 2007).

2.2. Image acquisition and pre-processing

The S2A and WV3 images were acquired for the summer of 2016–7 (Table 1) to coincide with the field campaign dates. Images for Hogsback were acquired in the 35S Universal Transverse Mercator (UTM) projection, whereas the S2A images for Tevredenpan were acquired in UTM36S, and the WV3 images in a geographic coordinate system. The 10- and 20-m bands of the S2A images were used (European Space Agency, 2019b; Supplementary material I; Table I.1). WV3 has eight bands in the visible to NIR regions of the EMS at 1.24 m, with an additional eight bands in the SWIR at 3.7 m (Supplementary material I; Table I.2). For the Hogsback area, multispectral WV3 data were obtained at the full extent of the study area, while only the western and central portion (6 263.5 ha or 75%) of the study area had a set of WV3 SWIR bands, which was then used for the WV3 analysis. For Tevredenpan, only multispectral WV3 images were afforded.

S2A and WV3 images that had less than 10% clouds were selected from the middle to end of the peak of the hydroperiod in the Grassland Biome (i.e., summer to late summer). Sentinel-2 images were acquired at the 1C processing level which included orthorectification. The Sen2Cor algorithm, available through the ESA's SeNtinel APplication Platform (SNAP; ESA, 2019a), was used to atmospherically correct multispectral S2A images. The algorithm parameter was chosen based on the location and type of environment of each study site in conjunction with the values recommended in the Sen2Cor configuration and user manual (Mueller-Wilm, 2017). The WV3 images were corrected using Atmospheric and Topographic Correction (ATCOR) to calibrate them to top-of-canopy reflectance using sensor and solar inclination and azimuth angles (Richter and Schläpfer, 2015). Canopy spectra for water, vegetation, and soil were used as input parameters and were related to reference spectra in ATCOR for the WV3 images.

2.3. Field campaigns and the identification of representative wetland vegetation groups

Each study area was visited at least twice when the vegetation was in full vigor and at peak productivity. Hogsback was initially visited from November 6 to 7, 2016, with subsequent fieldwork trips undertaken 13–17 February 2017 and again 19–23 February 2018. Tevredenpan was visited February 27 to March 2, 2017 and again 5–9 March 2018. At least a third of the patches sampled during the 2017 field campaign was revisited during the 2018 field campaign to assess the level of changes and species turn-over since the previous growth season. The extent of patches, structure and species composition were compared to the notes of the 2017 campaign. In all instances we concurred that patches showed no species turn-over nor changes in extent, structure and species composition, and therefore continued to use the patches identified in the 2016 (for Hogsback) and 2017 (both study area) campaigns.

Dominant vegetation communities were identified in the field, taking the communities defined through cluster analysis in the National Wetland Vegetation Database (Sieben et al., 2014) into account. This database identified 11 floristic wetland vegetation community

types (grouped to 10 floristic communities and three larger groups) from the cluster analysis for Hogsback and 19 for Tevredenpan (grouped to 13 floristic communities and six larger groups) (Supplementary material III, Table III.1).

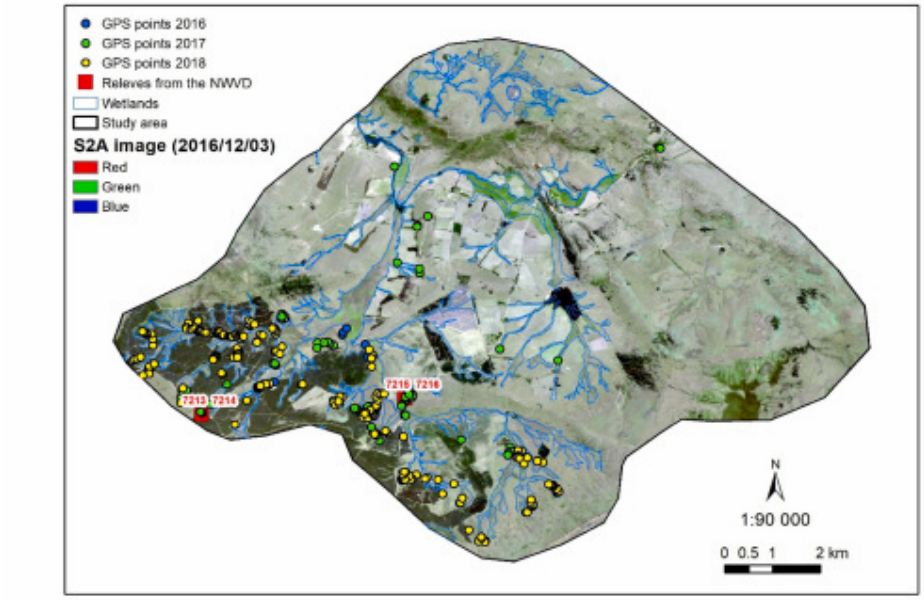

(A)

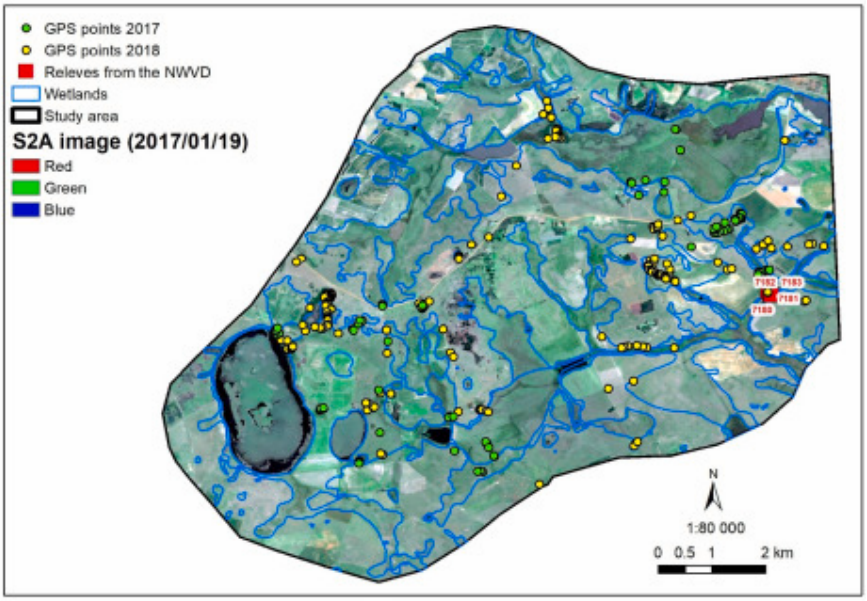

(B)

Fig. 2. Location of field floristic samples (relevés, red squares and red labels) and sample points (yellow and green circles) collected over two field campaigns, against the Sentinel-2 image false-color image using bands 2, 3 and 4 as blue, green and red bands, respectively of (A) Hogsback (dated to 2016/12/03); and (B) Tevredenpan (dated to 2017/01/19) study areas. The extent of wetland polygons shown here were mapped by wetland experts through heads-up digitizing.

Table 2. Comparison of wetland vegetation communities for remote sensing classification of the Hogsback and Tevredenpan study areas against those of the South African National Wetland Vegetation Database (NWVD) Sieben et al. (2014) [a].

Study area	Type	Wetland Vegetation Community	Relationship to vegetation communities from the NWVD	2016	2017	2018	Total
Hogsback	Aquatic	*Phragmites australis*[c]	[Points were not collected in the field; difficult to access].	0	0	0	0
	Aquatic	*Carex acutiformis*	*Carex acutiformis* (CG6.2).	1	10	34	45
	Aquatic	Mixed grass community	Elements of the following communities (i.e., these species at least) were all present: *Aristida junciformis* and *Tristachya leucothrix* (CG5.15), *Merxmuellera macowanii* (CG5.1), *Festuca caprina* (CG5.14), and *Haplocarpha nervosa* (CG5.11).	1	10	12	23
	Aquatic	Mixed sedge community	Elements of the following communities (i.e., these species at least) were all present: *Fingerhuthia sesleriiformis* (CG5.4), *Isolepis angelica* (CG5.2) and *Juncus inflexus* (CG5.9)	0	6	49	55
	Aquatic	*Ficinia nodosa*	Not assessed in the same way as Sieben et al. (2014) whereby this species would be included in a Braun Blanquette plot and incorporated into the community, not singled out as an individual	0	3	19	22
	Aquatic	*Imperata cylindrica*	Not assessed in the same way as Sieben et al. (2014) whereby this species would be included in a Braun Blanquette plot and incorporated into the community, not singled out as an individual	0	6	6	12
	Aquatic	Some patches were observed in disturbed sites, not considered sufficient in areal extent for spectral signature assessment	*Juncus effusus* (CG5.9)	0	0	8	8
	SUBTOTAL NR OF GPS PNTS FOR HOGSBACK			**2**	**35**	**128**	**165**

Tevredenpan	Terrestrial[b]	*Eragrostis plana* and *Themeda triandra*	>60% *Eragrostis plana* and *Themeda triandra*	0	15	12	27
	Aquatic[b]	*Aristida* spp. (>50%)	>50% *Aristida* spp.	0	13	3	16
	Aquatic[b]	*Arundinella nepalensis* (>50%)	*Arundinella nepalensis* (>50%)	0	20	3	16
	Aquatic	*Carex* spp. (>70%)	*Carex* spp. (>70%)	0	3	0	3
	Aquatic[b]	Grass-sedge communities	*Aristida junciformis* (±10%); *Arundinella nepalensis* (±20%); *Calamagrostis epigejos* (±20%); *Commelina africana* (±25%); *Cyperus denudatus* (±10%) and *Paspalum dilatatum* (±5%).	0	7	14	21
	Aquatic	*Juncus effusus* (>50%)	>50% *Juncus effusus* (CG6.4)	0	5	3	8
	Aquatic[b]	*Phragmites australis*[c]	>90% *Phragmites australis*	0	0	0	0
	Aquatic[b]	Sedge dominant (>20%)	±80% *Eliocharis dregreana* (CG6.1); ±16% *Leersia hexandra* (CG6.1) and <6% open water	0	8	3	26
	Aquatic[b]	Wet-grass communities	±70% *Cymbopogon validus with* < 10% of *Cyperus haematocephalus*; *Cyperus denudatus*; *Kylinga erecta*; *Leersia hexandra* (CG6.1) and *Pennisetum thunbergi*	0	5	36	41
	SUBTOTAL NR OF GPS PNTS FOR TEVREDENPAN			**0**	**92**	**72**	**164**
TOTAL NR OF GPS PNTS FOR BOTH STUDY AREAS				**2**	**127**	**200**	**329**

[a]Although the National Wetland Vegetation Database also indicated the *Arundinella nepalensis* community, only a sparse number of patches were observed on the floodplain fringe, and found to be insufficient in cover to be considered as a community that can be detected by the selected sensors of this study.
[b]Dominant in the landscape.
[c]Emergent vegetation was not always accessible on foot, and therefore canopy spectra were extracted at a desktop level.

Six to eight classes of wetland vegetation communities were initially selected for the remote sensing classification of the Hogsback study area (Table 2). Although additional patches were identified, they were considered too small or not representative in the study area for mapping with remote sensing images (Table 2). Approximately 165 locations were visited within the maximum eight days of fieldwork over a period of two summer seasons (Table 2; Fig. 2A). For some patches, the edges were also marked with a Garmin 62s GPS (spatial horizontal accuracy <5m); however, these edge points were not included in the points listed in Table 2. A total of 66 species were compiled following the addition to the list of species compiled by Janks (2014).

For the Tevredenpan study area, a total of 164 locations were visited within the maximum eight field days of fieldwork over a period of two summer seasons (Table 2; Fig. 2B). The 2017 and 2018 survey added 43 species to the list of the National Wetland Vegetation Database that was originally compiled by Linström (2014, 2015) and Mr. Hannes Marais of the Mpumalanga Tourism and Parks Agency (MTPA) in their previous surveys, totaling 192 species to date. From the groupings of the species, nine wetland vegetation communities for this remote sensing classification study were identified during the field surveys, one terrestrial and eight aquatic (Table 2). Seven of the wetland vegetation communities for the remote sensing classification were found to be prevalent and dominant in the landscape, while fewer locations of *Phr.* and *Carex* spp. were observed (Table 2). Dominant species were assumed to have a major influence on the reflectance within the pixel. Some monodominant species were easy to visually separate, for example, the wetlands dominated by grass or sedges, from *Juncus* spp. and *Phr. australis* (see Supplementary material III, Fig. III.1 as example).

2.4. Identifying regions of interest on the Sentinel-2 and WorldView-3 images and input layers

The center and edge GPS points collected during the field campaigns were used to inform the selection of Regions of Interest (ROIs), defined as a single extracted pure pixel of the target class, from the images. Care was taken to ensure that the pixels selected from the images, coincided with the center points of patches, and where relevant, were within the edge points collected. For Hogsback, a total of 13 ROI classes were captured, including one terrestrial, five palustrine, one lacustrine, two other natural and four modified (Supplementary material IV; Table IV.1). A minimum of 30 ROIs for each class was identified for Hogsback on both the S2A and WV3 images, except for the bare soil and woody invasive *Rubus* spp. classes, where only 20 and 14 ROIs could be captured, respectively. For Tevredenpan, 13 ROI classes were also captured, including one terrestrial, eight palustrine, one lacustrine, one other natural and two modified classes, with a minimum of 25 ROIs mapped for both S2A and WV3 images (Supplementary material IV; Table IV.2). The canopy spectra (see Supplementary material V) were exported to a comma separated value file (*.csv) file using the Environment for Visualizing Images (ENVI) 5.2 64-bit software (Exelis Visual Information Solutions Pty Digital Globe Pty Ltd, 2014).

Sample points of vegetation classes in Hogsback, which appeared distinct in the field, were also scrutinized visually on the WV3 images. Samples were considered unsuitable for mapping at image level if either fewer than five patches were recorded in the field in the

study area, or the diameter was ≤10 m, which would risk interference by reflectance from adjacent patches that are not similar. Consequently, several samples were excluded, namely *Imperata cylindrica*, *T. capensis*, *Schoenoplectrus brachyceras*, as well as other terrestrial and invasive species such as Bracken fern (*Pteridium aquilinum*), *Leucosidea sericea,* and Poplar trees (*Populus* spp.). *Isolepis cernue* dominated the canopy for one patch observed in the field, whereas in most of the other patches it was not dominant and was therefore included in the sedge class.

2.5. Comparison of classification scenarios

Five classification scenarios were compared to evaluate the optimization of separability of wetland and terrestrial vegetation, or wetland vegetation communities:

- Bands;
- Bands and elevation data: using a DEM;
- Bands and spectral indices;
- Bands and Above-Ground Biomass (AGB); and
- Bands, elevation, spectral indices, and AGB.

Elevation data were also considered in the classification scenarios because some wetland vegetation communities may be associated with higher-lying seeps compared to lower-lying valley-bottom wetlands. Therefore, a Digital Elevation Model (DEM) was built using the ArcGIS 10.3 Topo-to-raster tool (ESRI, 1999–2016), using the 5-m interval contours and 1:10 000 spot height data from the Department of Rural Development and Land Reform: National GeoInformation (DRDLR:NGI, 2016) as input data sets. The DEM was built to match the 10-m spatial resolution of the Sentinel-2A image pixels, and no hydrological correction was made to the DEM. For the WV3 classifications, the DEM was resampled to 3.7 m for Hogsback, according to the spatial resolution of the SWIR bands' spatial resolution, and 1.24 m for Tevredenpan, according to the spatial resolution of the multispectral bands. Where only one pixel was used for an ROI, the center-point of the pixel was used in shapefile format to extract the elevation value from the DEM. For ROIs consisting of more than one pixel of the image, a zonal mean value was extracted using the polygon extent of the ROI in ArcGIS 10.3.

Four vegetation indices and one leaf water content index were used to enhance the discrimination of biochemical and biophysical plant properties in the classification (Table 3). The inclusion of the four vegetation indices has previously shown some improvement in the OA of wetland tree species in a subtropical-temperate region of South Africa (Van Deventer et al., 2019), but it remains to be assessed for the Grassland Biome. These indices were applicable to the spectral bands of both S2A and WV3.

Where the Green, Red, Red Edge and near infrared (NIR) bands used in the indices correspond to bands 3, 4, 6 and 8 of the Sentinel-2 images, with the narrow-band NIR

Table 3. Spectral indices used to evaluate the change in the overall and average user's accuracies of all seasonal classification models.

Spectral Index	Equation	Plant property highlighted
Green Normalized Difference Vegetation Index (gNDVI) (Gitelson et al., 1996)	$gNDVI = \frac{(\mathrm{NIR} - \mathrm{Green})}{(\mathrm{NIR} + \mathrm{Green})}$	Chlorophyll
MERIS terrestrial chlorophyll index (MTCI); (Dash and Curran, 2004)	$MTCI = \frac{(\mathrm{NIR} - \mathrm{Red\ Edge})}{(\mathrm{Red\ Edge} - \mathrm{Red})}$	Chlorophyll
Normalized Difference Vegetation Index (NDVI); (Rouse et al., 1973; Tucker, 1979)	$NDVI = \frac{(\mathrm{NIR} - \mathrm{Red})}{(\mathrm{NIR} + \mathrm{Red})}$	Chlorophyll
Normalized Difference Water Index (NDWI) (Gao, 1996)	$NDWI = \frac{(RNIR - RSWIR)}{(RNIR + RSWIR)}$	Leaf water content
Red Edge Normalized Difference Vegetation Index (NDVIre); (Gitelson and Merzlyak, 1994)	$NDVIre = \frac{(\mathrm{NIR} - \mathrm{Red\ Edge})}{(\mathrm{NIR} + \mathrm{Red\ Edge})}$	Chlorophyll, leaf area/biomass and nitrogen

(band 8A) and SWIR1 bands used for NDWI; for the WorldView-3 images, bands NIR2 were used as well as SWIR1 for NDWI.

Lastly, AGB was considered an important variable with wetland and terrestrial vegetation communities showing a variety of vegetation height and density (visual observations in the field). AGB for the two study areas were calculated by Naidoo et al. (2019). This study incorporated field-based Leaf Area Index measurements together with Sentinel-1 backscatter (Vertical-Horizontal and Vertical-Vertical), Sentinel-2 optical reflectance bands, spectral vegetation indices, and band ratios, within a bootstrapped Random Forest modelling environment (with variable important selection), to estimate AGB.

2.6. Analysis of the separability between classes for SDG 6.6.1a reporting, and at vegetation community level using canopy spectra and images

The separability of wetland vegetation was done at three levels for the first three objectives (Fig. 3). First, we assessed the capabilities of the classification scenarios to distinguish wetland vegetation from terrestrial vegetation. This would contribute to improved reporting to SDG 6.6.1a, where the extent of the lacustrine and palustrine biomes of wetlands are required from countries. For this purpose, only the respective canopy spectra (Table 4, Table 5) were grouped into two classes as either palustrine or terrestrial vegetation, and then analyzed in the Waikato Environment for Knowledge Analysis (Weka) software version 3.8 (Franke et al., 2016). A 100-fold cross-validation approach was used to test possible errors and determine the overall, producer's and individual user's accuracies that could be achieved from the ROIs. For this purpose, the ROI classes were subsequently classified with the Random Forest algorithm (Breiman, 2001) using the various options of bands, elevation, spectral indices, and AGB input variables. Random Forest is a non-parametric classifier often used for species separability (Naidoo et al., 2012; Dubeau et al., 2017; Van Deventer et al., 2017; Beyer et al., 2019; Van Deventer et al., 2019a).

Second, we evaluated the separability between different wetland and terrestrial vegetation communities for purposes of monitoring (Fig. 3). For this level of analysis, the canopy spectra of all classes were evaluated in a cross validation approach, using the five classification scenarios with respective input layers. The variances in errors were calculated based on the best-practice guidelines of Olofsson et al. (2013, 2014). Each of the models was predicted in R Studio (R Core Team, 2009–2021) using the ModelMap package (Freeman and Frescino, 2009). Subsequently, the images were converted to polygons (no smoothing) in ArcMap version 10.3 (ESRI, 1999–2016) and the areal extent calculated in hectares (ha) using the Albers Equal Area Conical projected coordinate system of South Africa. This coordinate system least distorts the surface area of polygons (Waywell, 2009), and uses the World Geodetic System of 1984 (WGS84) with the 25°E central meridian and 24°S and 33°S as standard parallels. The total areal extent of each class was then used to update the accuracies as per Olofsson et al. (2013, 2014).

In both the Weka and ModelMap assessments, the software defaults of *ntree* (=500) and the *mtry* variable (i.e., square root of the number of input variables) were retained. The *mtry* variable varied according to the number of variables in the classification scenarios and according to the optimizations of splits at the nodes in the trees. The optimal classification scenario for each study area and the sensor for separating at the coarser level between lacustrine wetlands, palustrine and terrestrial vegetation was identified using where the average OA was maximized and where the lowest user's accuracy for an individual class reached a maximum. For the classification at vegetation community level, the optimal classification scenario was selected where the adjusted OA reached a maximum, and the lowest adjusted user's accuracy of an individual class was maximized. We also considered the number of instances where comparable pairs were confused by >10% and aimed to minimize class confusion. Subsequent to the analysis, the optimal results were used to calculate the areal extent of each class, and also group these for SDG 6.6.1a reporting as the extent of lacustrine and palustrine wetlands, respectively. For the third objective the overall, producer and user's accuracies (Story and Congalton, 1986) attained from the various classification scenarios were compared to assess whether the use of ancillary data improved the classification accuracies (Fig. 3).

2.7. Evaluation of the contribution of the red edge and SWIR bands in separating vegetation classes

Lastly, for the fourth objective, we used a subset of the ROIs, consisting only of the vegetation classes of each study area (omitting bare soil and open water), to evaluate the importance of the red-edge and SWIR bands for enhancing separability between them (Fig. 3). Accuracies were calculated using the Random Forest algorithm in Weka with a 100-fold cross validation approach, first using all the spectral bands of each sensor, and subsequently after removing first the SWIR bands, and thereafter the red edge band(s) as well. Changes in the average OA and lowest average UA were used to compare the impact of removing the spectral bands on the classification accuracies. Removing the SWIR bands from the WV3 image of Hogsback, makes this classification comparable to that of WV2, giving a glimpse on the improved capabilities of WV3 with the SWIR bands.

3. Results

3.1. Wetland and terrestrial vegetation are highly separable in the Hogsback and Tevredenpan study areas

Wetland and terrestrial vegetation were found to be highly separable, with the average OAs 91–99% and the individual user's accuracies 88–99% for both sensors and study areas (Table 4). The S2A classification scenarios showed a 0–4.7% difference in the average OAs reported for Hogsback and 0–0.8% difference for Tevredenpan, while the average OA achieved by WV3 for the two study areas was 0–7.1% and 0–1.4%, respectively. For the Sentinel-2 and WV3 sensors, the lowest average user's accuracies between the comparable classification scenarios differed by ≤ 4.7% and ≤7.4% for Hogsback, respectively, and ≤4.6% and ≤7.7% for Tevredenpan, respectively.

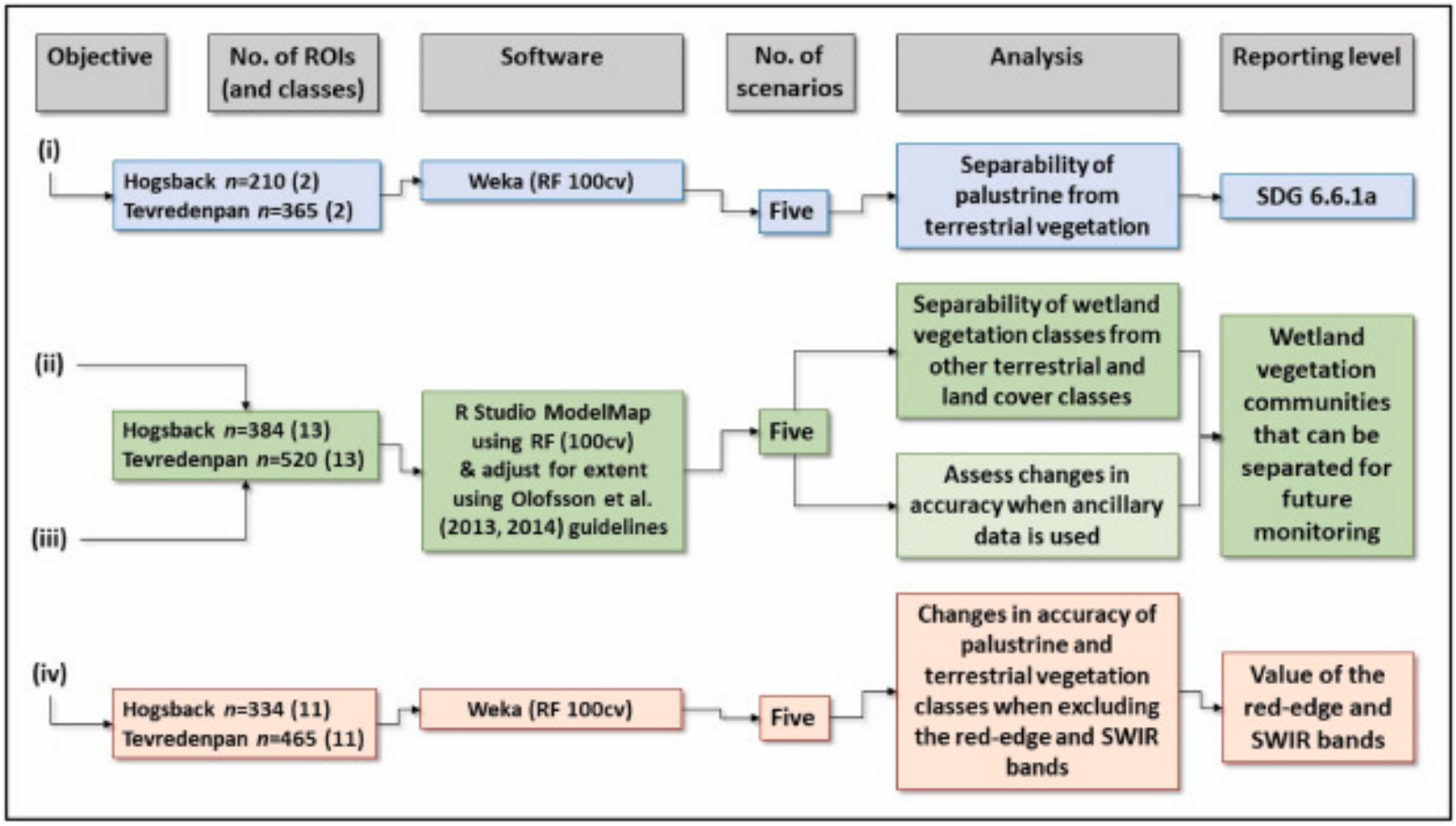

Fig. 3. Flow diagram showing the relationship between the four objectives of the study, the number of regions of interest (ROIs), the number of classes, the software and classification scenarios used for the analysis, the type of analysis and the intended level of reporting. cv = cross validation; RF = random forest algorithm; SDG = Sustainable Development Goal; SWIR = shortwave infrared. Objectives and related processes are color coded according to their associated reporting level. The five classification scenarios include (a) bands; (b) bands and elevation data; (c) bands and spectral indices; (d) bands and above-ground biomass (AGB); and (e) bands with elevation, spectral indices and AGB data.

Table 4. Variances in the average overall and lowest user's accuracies (OA, UA) of the classification scenarios that distinguish between wetland and terrestrial vegetation for the Tevredenpan and Hogsback study areas. Figures in bold indicate the optimal modelling scenario where the average OA and lowest UA were maximized for a sensor and study area. Classification scenario abbreviations: AGB - Above-ground biomass. Band ranges: from the VNIR (visible to near infrared) to the SWIR (shortwave infrared).

	Hogsback		Tevredenpan	
	S2A (VNIR-SWIR)	WV3 (VNIR-SWIR)	S2A (VNIR-SWIR)	WV3 (VNIR)
Number of samples:	Palustrine $n = 150$; Terrestrial $n = 60$[a].	Palustrine $n = 150$; Terrestrial $n = 60$[a].	Palustrine $n = 310$; Terrestrial $n = 55$	Palustrine $n = 310$; Terrestrial $n = 55$
Overall accuracy (%)				
Bands	91.0	91.9	93.7	95.6
Bands & elevation	93.3	93.3	**94.5**	95.9
Bands & indices	93.8	98.6	93.7	95.9
Bands & AGB	91	94.8	93.7	95.3
Bands, elevation & indices	**95.7**	**99.0**	94.0	**96.7**
Bands, elevation, AGB & indices	95.2	98.6	94.0	96.4
Lowest user's accuracy (%)				
Bands	90.2	91.3	88.1	88.2
Bands & elevation	92.5	92.0	**92.7**	90.0
Bands & indices	93.1	98.0	90.0	91.7
Bands & AGB	90.7	93.7	88.1	88.0
Bands, elevation & indices	**94.9**	**98.7**	90.2	**95.7**
Bands, elevation, AGB & indices	94.3	98.0	90.2	95.7

[a]Includes the Eragrostis-Themeda-Andropogon spp. or 'ET' class and the Mountain Slopes class.

Including ancillary data (elevation, spectral indices, and AGB) increased the average OA by up to 5% for S2A and 7% for WV3 in the Hogsback study area. For Tevredenpan, however, the inclusion of these ancillary datasets improved the OA by 1% for S2A and 1.4% for WV3. The lowest average user's accuracies showed increases similar to those of the average OA for Hogsback when ancillary data were included in the classification scenarios (5% and 7% for S2A and WV3, respectively), while increases of 5% for S2A and 8% for WV3 were observed for Tevredenpan.

3.2. Separability of wetland vegetation communities for Hogsback and Tevredenpan and contribution of ancillary data to classification

In general, the spectra of the vegetation classes, consisting of a mixture of vegetation communities, monodominant species, and plant functional types, proved to be highly separable (Table 5). For both sensors, the average OA was between 64% and 69% for both study areas. For WV3, the average OA improved by 2% compared to S2A for the bands-only classification scenario for Hogsback, however, showed a 10% decrease in average OA compared to the band-only classification result of S2A for Tevredenpan, owing to the lack of SWIR bands for this area.

When considering the use of ancillary data (elevation, spectral indices, and AGB), the average OA improved by 11% for S2A and 15% for WV3 in the Hogsback study area and by 4% for S2A and 10% for WV3 in Tevredenpan when all ancillary data were included in the classification scenarios (Table 5). The lowest average individual user's accuracy also improved for all sensors and study areas when ancillary data was used in addition to the bands in the classification scenarios, with an improvement of up to 16.6% for S2A and 7.1% for WV3 in Hogsback, and up to 4% for S2A and 8% for WV3 in Tevredenpan. The optimal classification scenario for all sensors and study areas was where the bands and all ancillary data were used, except for Tevredenpan in the S2A classification, where the use of the bands-and-elevation and bands-with-all-ancillary-data scenarios both attained an average adjusted OA of 78.6%, but the lowest average UA was maximized at 56% in the bands-and-elevation scenario, compared to UA = 52% in the bands-with-all-ancillary-data scenario (bold figures, Table 5). Using all ancillary data with the spectral bands also reduced the number of classes with >10% of class confusion, compared to using the spectral bands only (Table 5; Supplementary material VI).

In Hogsback, the vegetation classes predicted from S2A that showed the highest percentage of overlap were *Ficinia* spp. (FS), *Merxmuellera macowanii* (MM), sedge-dominant class (SE) and terrestrial vegetation community classes (Supplementary material VI; Table VI.1), while *Carex* spp. (CA) showed an overlap with crops (CR). The sedge-dominant class showed the lowest average adjusted UA and PA of 53.3%. The percentage of overlap and number of spectrally confused classes are slightly reduced when using the WV3 optimal classification scenario (Supplementary material VI; Table VI.2). The lowest average adjusted UA was for the *Rubus* spp. (RS), attaining 50%, while the lowest average adjusted PA was 61% for *Ficinia* spp. For Tevredenpan in the S2A optical classification scenario, a spectral overlap of >10% was observed for the *Arundinella nepalensis* (AR), *Aristida* spp. (AS), grass-sedge (GS), sedge-dominant (SE) and wet-grass (WG) communities, with the sedge-dominant class attaining the lowest average adjusted UA of 56% and PA of 42% (Supplementary material VI;

Table 5. Variances in the adjusted average overall and lowest user's accuracies (OA, UA) of the test data sets from the Hogsback and Tevredenpan study areas using Sentinel-2A (S2A) and WorldView-3 (WV3) images for detailed vegetation community classes and other cover classes. The average accuracy was achieved using a 100-fold cross-validation approach, with values adjusted for surface area predicted, as per the best practice guideline of Olofsson et al. (2013, 2014). Values in bold indicate the optimal classification scenario where both the adjusted average OA and lowest UA are both maximized. Classification scenario abbreviations: AGB - Above-ground biomass. Band ranges: VNIR - visible to near infrared, SWIR - shortwave infrared. Abbreviations for individual classes under the UAs are: BA = Bare soil; AN = *Arundinella nepalensis*; CA = *Carex* spp.; FS = *Ficinia* spp.; GS = Grass-sedge communities, MM *Merxmuellera macowanii*; PA = *Phragmites australis*; RS = Invasive tree species (woody); and SE = sedge-dominant communities (see Supplementary material IV, Tables IV.1 and IV.2 **for** the full list of communities used.

Study area:	Hogsback		Tevredenpan	
Sensor:	S2A (VNIR-SWIR)	WV3 (VNIR-SWIR)	S2A (VNIR-SWIR)	WV3 (VNIR)
Number of samples (and classes) per broad categories:	Palustrine $n = 150$ (5); Lacustrine $n = 30$ (1); Other $n = 144$ (5); Terrestrial $n = 60$ (2)	Palustrine $n = 150$ (5); Lacustrine $n = 30$ (1); Other $n = 144$ (5); Terrestrial $n = 60$ (2)	Palustrine $n = 310$ (8); Lacustrine $n = 30$ (1); Other $n = 125$ (3); Terrestrial $n = 55$ (1)	Palustrine $n = 310$ (8); Lacustrine $n = 30$ (1); Other $n = 125$ (3); Terrestrial $n = 55$ (1)
Overall accuracy (%)				
Bands	61.0	68.8	74.2	64.1
Bands & elevation	74.0	76.0	**78.6**	71.5
Bands & indices	70.3	78.1	62.7	63.2
Bands & AGB	65.6	76.0	73.8	68.0
Bands, elevation & indices	77.5	80.3	77.2	71.9
Bands, elevation, AGB & indices	**78.2**	**83.3**	78.4	**73.8**
Individual user's accuracy in %				
Bands	36.7 (SE)	42.9 (RS)	52.0 (AN)	40.0 (GS)
Bands & elevation	46.7 (SE)	46.7 (FS)	**56.0 (AN)**	48.0 (AN)
Bands & indices	36.7 (FS)	46.7 (FS)	36.0 (AN)	36.0 (AN)
Bands & AGB	30.0 (SE)	35.7 (RS)	36.0 (AN)	46.0 (GS)
Bands, elevation & indices	53.3 (FS, SE)	43.3 (FS)	56.0 (AN)	44.0 (AN)
Bands, elevation, AGB & indices	**53.3 (SE)**	**50.0 (RS)**	52.0 (AN)	**48.0 (AN)**
Individual producer's accuracy in %				
Bands	32.1 (FS)	45.8 (MM)	45.8 (AN)	30.4 (AR)
Bands & elevation	35.4 (FS)	50.5 (FS)	41.9 (SE)	45.1 (AR)
Bands & indices	33.1 (PA)	52.2 (MM)	20.3 (SE)	24.4 (CA)
Bands & AGB	33.0 (SE)	55.6 (FS)	37.8 (BA)	28.6 (AR)
Bands, elevation & indices	45.4 (SE)	58.9 (FS)	24.4 (SE)	39.7 (AR)
Bands, elevation, AGB & indices	47.7 (FS)	61.2 (FS)	29.2 (SE)	50.4 (SE)
Number of comparable pairs showing confusion > 10% of the total number of reference ROIs				
Bands	14	13	6	19
Bands & elevation	9	8	6	11
Bands & indices	11	7	16	18
Bands & AGB	10	6	6	15
Bands, elevation & indices	7	5	5	9
Bands, elevation, AGB & indices	6	5	6	10

Table VI.3). The number of spectral classes, showing an overlap of >10%, increased from the S2A optimal classification compared to the WV3 optimal classification, which can be attributed to the limited number of spectral bands available (Supplementary material VI; Table VI.4). The wet-grass (WG) class showed the highest number of overlaps with other classes, although the *A. nepalensis* (AR) class attained the lowest average adjusted UA of 48% while the sedge-dominated class (SE) had the lowest PA of 50%.

The resultant maps for Hogsback are shown in Fig. 4 and for Tevredenpan in Fig. 5. For the Hogsback study area, the extensive reed bed along the Klipplaatsriver (*Phr. australis* or PA) is now clearly visible and an improvement in the land cover classes (Fig. 4 compared to Fig. 2A). The S2A map for Hogsback shows a more extensive cover and possibly an overestimation of *Ficinia* spp. and sedge-dominant classes in seeps and valley-bottom wetlands in the south, resulting from low accuracies (Fig. 4A). The areal extent of these classes is reduced in the WV3 map for Hogsback (Fig. 4B). Similar to the Hogsback study area, the areal extent of *Phr. australis* (PA) are clearly discernible in the large depressional wetland called 'Tevredenpan' in the west of the study area, and Kleinpan in the south-east of it, and an improvement in the land cover map for the area (Fig. 5 compared to Fig. 1F). It was interesting to observe how extensive wet grasses are in the study area, dominating the east-west valley-bottom wetland in the northern part of the study area, while the valley-bottom wetland running eastward in the southern part, is dominated by *Carex* spp. These classes appear to be more extensive on the S2A map (Fig. 5A) compared to the WV3 map (Fig. 5B). The WV3 map also shows a large amount of salt-and-pepper effect, resulting from the pixel-based approach with a 1.24-m spatial resolution.

3.3. Contribution of the red-edge and SWIR bands to the separability of vegetation classes

Excluding the SWIR bands in the classification of vegetation, result in a decrease of 0–2.6% in the OA for the Sentinel-2A sensor for the two study areas (Table 6). Omitting the SWIR bands from the WV3 classification in Hogsback, decreased the OA by 4.5%. When both the SWIR and red-edge bands are omitted from the S2A classification of both study areas, the OAs decrease by 4.8–7.3%, while for the WV3 classification of Hogsback, the decrease in OA was 1.5%. When the red-edge band is omitted from the WV3 VNIR classification in Tevredenpan, the OA increases by 5.3%. Interestingly, the lowest average UAs for Hogsback was attained when the SWIR and/or red-edge bands were omitted from S2A and WV3, while the use of all spectral bands of S2A maximized the lowest average UA to 60% for the S2A sensor.

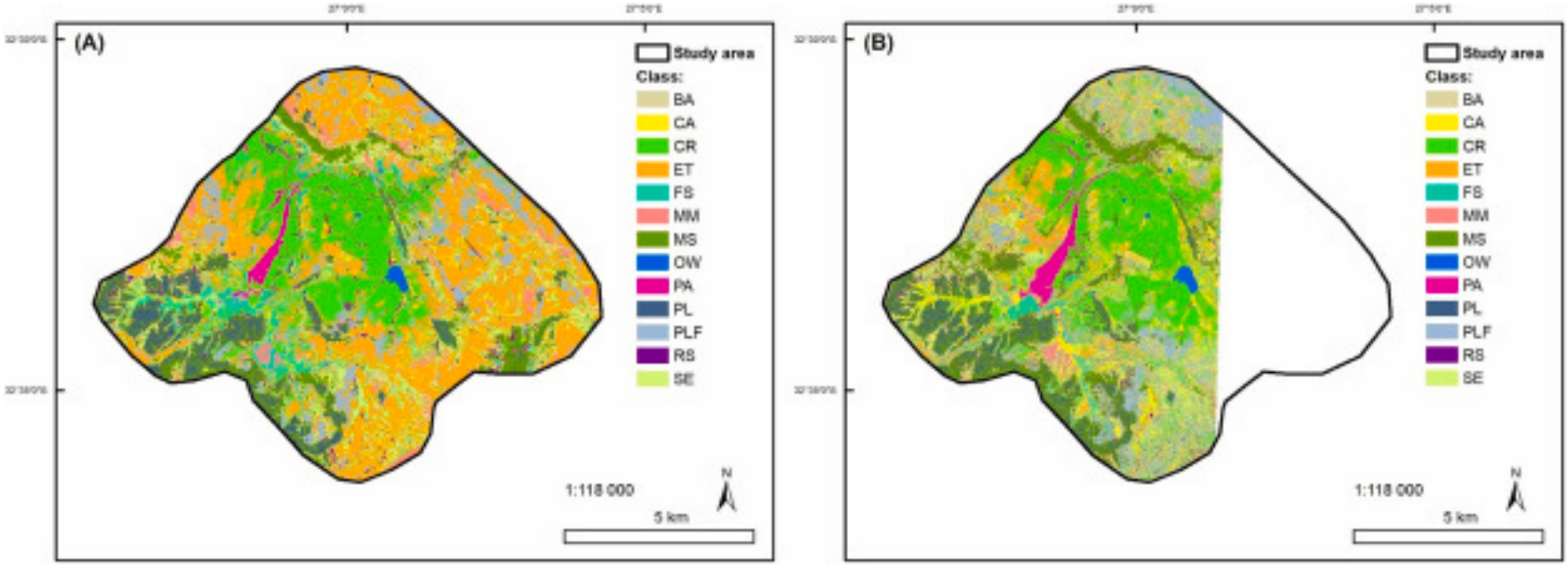

Fig. 4. The predicted extent of wetland vegetation communities and other classes for the Hogsback study area was derived from (A) the Sentinel-2 bands and ancillary data; and (B) the WorldView-3 bands-and-all-ancillary data. *BA = Bare soil; CA = Carex* spp.*; CR = cropland; ET = Eragrostis* spp. *and Themeda* spp.*; FS = Ficinia* spp.*; MM = Merxmuellera macowanii; MS = mountain slope; OW = open water; PA = Phragmites australis; PL = plantations; PLF = plantations felled; RS = Rubus* spp.*; SE = Sedge dominant.*

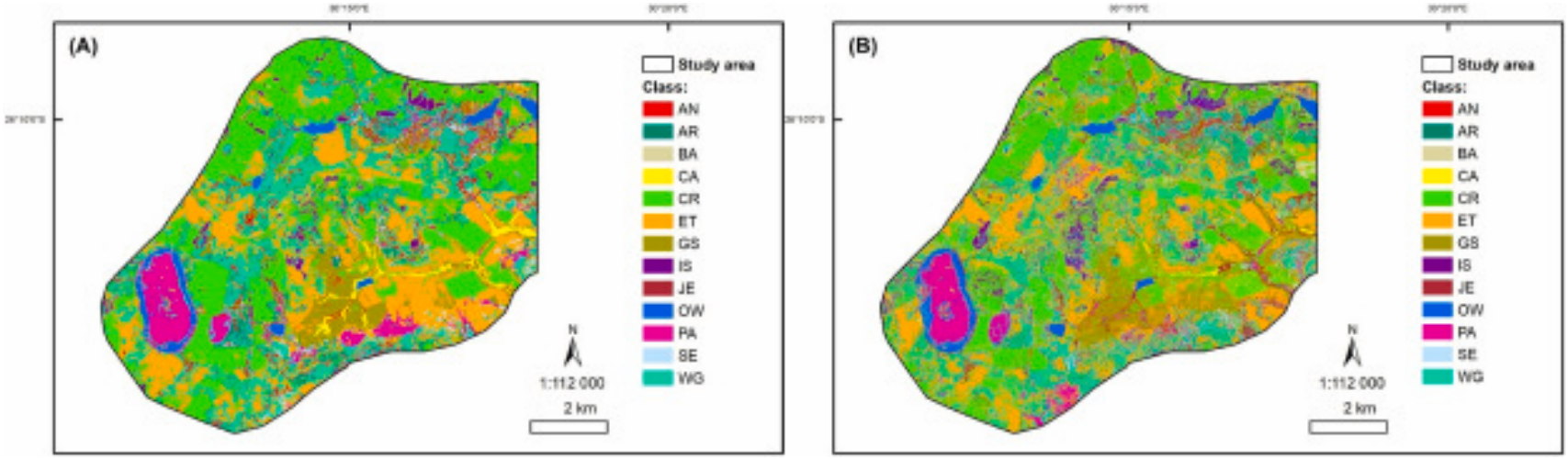

Fig. 5. The predicted extent of wetland vegetation communities and other classes for the Tevredenpan study area derived from (A) the Sentinel-2 bands and elevation data; and (B) the WorldView-3 bands and ancillary data. Abbreviations: AN = *Arundinella nepalensis*; AR = *Aristida* spp.; BA = bare soil; CA = *Carex* spp.; CR = cropland; ET = *Eragrostis* spp. and *Themeda* spp.; GS = grass-sedge communities; IS = invasive species; JE = *Juncus effusus*; OW = open water; PA = *Phragmites australis*; SE = Sedge dominant; WG = Wet-grass.

Table 6. Average accuracies resulting from using all spectral bands of the sensors in the 100-fold cross-validation of vegetation classes (no bare soil or open water) for the Hogsback and Tevredenpan study areas. Abbreviations: S2A = Sentinel-2A; WV3 = WorldView-3.

Study area:	Hogsback		Tevredenpan	
Sensor:	S2A (VNIR-SWIR)	WV3 (VNIR-SWIR)	S2A (VNIR-SWIR)	WV3 (VNIR)
Number of samples (and classes) per broad categories:	Palustrine $n = 150$ (5); Other $n = 124$ (4); Terrestrial $n = 60$ (2)	Palustrine $n = 150$ (5); Other $n = 124$ (4); Terrestrial $n = 60$ (2)	Palustrine $n = 310$ (8); Other $n = 100$ (2); Terrestrial $n = 55$ (1)	Palustrine $n = 310$ (8); Other $n = 100$ (2); Terrestrial $n = 55$ (1)
Overall accuracy (%)				
All spectral bands	**65.3**	**70.7**	**75.5**	N.A.[a]
Excluding the SWIR bands	65.3	66.2	72.9	**60.9**
Excluding SWIR and red-edge bands	60.5	69.2	68.2	66.2
Individual user's accuracy (%)				
All spectral bands	28.6	**50.0**	**60.0**	N.A.[a]
Excluding the SWIR bands	**35.7**	44.0	52.6	**40.4**
Excluding SWIR and red-edge bands	33.3	**50.0**	43.8	36.0

[a]Not afforded for this project.

4. Discussion

4.1. SDG 6.6.1a reporting: palustrine wetlands are highly separable using S2A and WV3 for two study areas in the grassland biome of South Africa

The wetland vegetation spectra extracted from the S2 images for the two ±8000 ha-extent study areas in the Grassland Biome of South Africa were highly separable (maximum OA > 95% accuracy for the two sensors and study areas) from terrestrial vegetation. Comparable results in the separability of palustrine wetlands and terrestrial were achieved (OA > 82%) in the grasslands of Ethiopia, using Landsat and radar (ALOS PALSAR L-band backscatter) data, in single and multiple seasons (Dubeau et al., 2017). Palustrine wetlands are therefore highly separable from terrestrial grassland, and a number of sensors (Sentinel-2 and WV3 in our study, or Landsat) can be used to map and reporting to the areal extent, and potentially changes in the areal extent of palustrine wetlands to SDG 6.6.1a.

At the level of separation of palustrine wetlands from terrestrial grasslands, the WV3 classifications showed a marginal improvement compared to the S2 classification for both study areas by 2.2–3.3% in the average OA, while the accuracies of individual classes with the lowest average UA increased by 3–3.8%. Inclusion of ancillary data improved the average OA by 0.8–7.1% for both sensors and study areas, while the accuracies of individual classes with the lowest average UA increased by 4.6–7.5%. Improvements in the separability of wetland and terrestrial vegetation were also observed through the inclusion of elevation and spectral indices as ancillary data for the Ethiopian study (Dubeau et al., 2017).

4.2. Palustrine wetland subtypes could be mapped with both S2A and WV3

Both the S2A and WV3 classifications showed capabilities in separating vegetation classes from each other and from other land cover classes, with the average adjusted OAs of the various classification scenarios ranging from 61% to 83%. In Hogsback we managed to separate five palustrine wetland classes from terrestrial and other land cover classes (totaling 13 classes), while in Tevredenpan eight palustrine wetland classes were mapped. When the sensor results are compared, WV3 with the VNIR to SWIR bands available for Hogsback had an average adjusted OA of 83.3% for the optimal classification, which is 5.1% higher than the OA achieved through the S2A optimal classification (OA = 78.2%). In contrast, for Tevredenpan, the optimal S2A classification was 78.6%, nearly 5% higher than the optimal classification achieved with WV3's VNIR bands. When the individual user's accuracies are considered between the sensors across the two study areas, the optimal Sentinel-2 classifications resulted in higher UAs for individual classes with the lowest average adjusted UA, by 3–8%. Classes that are generally grass and sedge-dominant, showed the highest degree of overlap in all classification scenarios, sensors, and study areas. Our results suggest that wetland vegetation communities are site specific and differ between catchments of the Grassland Biome of South Africa. Reporting changes in the species composition as an essential biodiversity variable for freshwater ecosystems (Turak et al., 2017) would require fine-scale monitoring. These initial classes proposed for our study areas, should be further assessed in a multi-temporal analysis change detection to determine suitability of reporting to targets for the post-2020 Global Biodiversity Framework (CBD, 2021).

Several other studies showed a high level of overlap or confusion between graminoid and sedge wetland vegetation, or otherwise also called 'marshland'. In Poland, the individual producer's and user's accuracies were 76–100% and 57–100% respectively, using WV2 images in a decision-tree classification of eight vegetation categories of which five were palustrine wetlands (Bochenek et al., 2013). In Ethiopia, grass and sedge wetland categories were found to be poorly separable, even when multiple seasons and additional indices were used to improve Landsat and the ALOS PALSAR L-band sensor classifications (Dubeau et al., 2017). The Ethiopian study used Landsat in the classification of 12 classes, and the lowest individual user's accuracies ranged from 72 to 95%, with the grass-marsh class achieving the lowest and highest percentage of UA under different classification models (Dubeau et al., 2017). A study in France also found spectral confusion between wetland vegetation communities, attributed to the presence of species in multiple communities (Rapinel et al., 2019). Another study in the Dube Delta, assessed the separability of 13 macrophyte classes using Sentinel-1, -2 and Pleiades data in combination with several indices. The models using only Sentinel-2 attained an OA > 75%, though a reduction on the OA when indices were included. A study in the grasslands of Germany, using a UAV, reported individual user's accuracies ranging from 40% to 65%, with the *Calamagrostis*, *Festuca*, *Glyceria,* and *Juncus* species classes showing the lowest accuracies (Beyer et al., 2019). The separability of 18 wetland vegetation communities or ecotypes across 13 predominantly palustrine wetlands in Ireland attained high OAs (84–87%), yet also showed spectral overlap between some classes, with individual user's accuracies<50% (Bhatnagar et al., 2020).

Monodominant classes such as the papyrus swamp forest and forested wetlands for the Ethiopian study, and the open water, *Phragmites*, *Carex,* and *Typha* spp. classes in the Great Lakes, Danube Delta and German study areas, showed high percentages of individual producer's and user's accuracies, compared to classes dominated by sedges and grasses (Bourgeau-Chavez et al., 2015; Dubeau et al., 2017; Beyer et al., 2019; Niculescu et al., 2020). Mapping and monitoring the increase in clonal and more resilient species such as *Phr. australis* and *Carex* spp. may therefore compare to other narrowly distributed wetlands, or marsh-like species. These large macrophyte classes would therefore be easy to map across various palustrine wetlands globally, serving as a third structural category under the TF1 Palustrine wetlands biome, of the International Union for Conservation of Nature's (IUCN's) global ecosystem types, supplementing the existing forested and marsh wetlands proposed (Keith et al., 2020, 2022).

The use of elevation and spectral indices as ancillary data with the spectral bands improved the OA and the lowest individual accuracies for both sites and sensors by OA = 4.4–17.2% and UA of 4–16.6%, while also minimizing the percentage confusion between comparable pairs. The use of ancillary data in the Ethiopian grasslands study also showed an increase in the OA of 1–4% and 2–8% when multi-seasonal information was used, and an increase of approximately 2% in the OA when a combination of optical and L-band backscatter images was used (Dubeau et al., 2017). For the Danube Delta, the inclusion of eight indices from Sentinel-2 resulted in a reduction of the OA by between 7 and 11%, in comparison to the Sentinel-2 bands only classification (Niculescu et al., 2020). In the German study, the value of adding elevation was measured as the most important variable to reduce error, whereas the inclusion of the blue, green, and red and thermal bands appeared to be less important,

although the effect of removing these variables on accuracies was not assessed (Beyer et al., 2019).

4.3. Value of the red-edge and SWIR bands for mapping palustrine wetland types

Our study assessed the impact of SWIR bands from Sentinel-2 images on the classification accuracy of wetland vegetation communities. Omitting the SWIR bands from the classification of vegetation classes, showed a decrease of 0–2.6% in the average OA for all study areas, but particularly for the Sentinel-2 classifications. When both the red-edge and SWIR bands were omitted in the Sentinel-2 classifications, a decrease in the average OA of 4.8–7.3% was observed, while it was only 1.5% lower in the classification of Hogsback using WV3. A study on the use of the red-edge band of RapidEye images in the classification of wetland tree species in a subtropical region of South Africa showed that this band increases the average OA by 2–6% (Van Deventer et al., 2019b). The incorporation of RE and SWIR bands in current and future sensors will help to continue to discriminate between distinct vegetation functional types from surrounding environmental elements.

5. Conclusions

This study showed that freely available Sentinel-2 images can effectively be used to separate wetland and terrestrial vegetation from each other in the Grassland Biome of South Africa, with an adjusted OAs of >91% in two study areas with Sentinel-2 and WorldView-2 images. This means that freely available Sentinel-2 images can potentially be used for improved mapping and reporting of changes in the geographic extent of palustrine wetlands in grassland biomes for SDG 6.

Furthermore, using both Sentinel-2 and WorldView-3 images, we were able to map between five and eight wetland vegetation communities or palustrine wetland subtypes. When using all the spectral bands with ancillary data, WV3 attained the highest average overall and user's accuracies, while Sentinel-2 with ancillary data were 5% lower in OA compared to the WV3 optimal classification. Grass and sedge communities remain spectrally confused, and class accuracies may be improved through grouping of classes to a combined “marshland” class. Further work is required using multi-temporal images to assess changes in the extent and possible degradation of these communities over time. The suitable classes for monitoring, the appropriate scale of monitoring, temporal interval, and reference dates remains to be assessed across various scales of sensors and the hydrological cycle.

The omission of the red-edge and SWIR bands, in general, resulted in a decrease in the average overall and user's accuracies, even though these bands were not always identified as the top priority bands in the variable importance ranks.

Funding information

The authors' time and resources were co-funded between April 1, 2016 and March 31, 2020 by (a) the Water Research Commission (WRC) for a project titled Establishing Remote Sensing Toolkits to Monitor Freshwater Ecosystems Under Global Change (Project No. K5/2545) and (b) the Parliamentary Grant Project of the Council for Scientific & Industrial

Research (CSIR) titled “Common Multi-Domain Development Platform (CMDP) to Realise National Value of the Sentinel Sensors for various land, freshwater and marine societal benefit areas”. Dr Van Deventer's additions during 2021 and 2022 were funded by the CSIR Parliamentary Grant Project titled “Research 2 Operational Pathways for Marine Observational and Predictive System Capabilities (MAROPS)”.

Disclaimer

The views and opinions expressed in this article are those of the author and do not necessarily reflect the official policy or position of any affiliated agency of the author.

Ethical statement

We as authors would like to declare that we have followed and adhered to all ethical practices in the development, writing, and publication of the article.

Author contributions(CRediT)

Dr Heidi van Deventer: Conceptualization, Data curation, Formal analysis, Funding acquisition, Methodology, Oversight and leadership, Project administration, Software, Writing of the original draft, Writing – integration of comments, Writing – review & editing, Remote sensing and GIS of wetland typing and classification. Mr Anton Linström: Investigation, Fieldwork, Data capturing, Expert on vegetation and wetland types related to the Mpumalanga Lakes District and Chrissiesmeer region of South Africa. Dr Laven Naidoo: Methodology, Software, Validation, Writing – review & editing, Expert on optical and radar classification of woody and wetland vegetation. Ms Nancy Job: Fieldwork, data capturing, Writing – review & editing, Expert on vegetation and wetland types related to the Hogsback study area in the Eastern Cape Province of South Africa. Dr Erwin Sieben: Fieldwork, Species identification, review & editing, Wetland vegetation types in Mpumalanga Lake District and Hogsback. Prof. Moses Cho: Writing – review & editing, Remote sensing expert on vegetation.

Declaration of competing interest

The authors declare that they have no known competing financial interests or personal relationships that could have appeared to influence the work reported in this paper.

Acknowledgements

We are grateful to the land owners who granted us access to their properties for sampling. The authors thank Dr Mervyn Lötter and Dr Mike Silberbauer who has done an initial review of the work and made suggestions for its improvement. We are also thankful to the reviewers who provided comments towards the improvement of this manuscript.

Data availability

Data will be made available on request.

References

Bailey, A.K., Pitman, W.V., 2016. Water Resources of South Africa, 2012 Study (WR2012). Book of Maps, Water Research Commission (WRC) Report No. TT 685/16, vol. 3. WRC, Pretoria, South Africa.

Beyer, F., Jurasinski, F., Couwenberg, J., Grenzdörffer, G., 2019. Multisensor data to derive peatland vegetation communities using a fixed-wing unmanned aerial vehicle. Int. J. Rem. Sens. 40 (24), 9103–9125.

Bhatnagar, S., Gill, L., Regan, S., Naughton, O., Johnston, P., Waldren, S., Ghosh, B., 2020. Mapping vegetation communities inside wetlands using Sentinel-2 imagery in Ireland. Int. J. Appl. Earth. Obs. Geoinf. 88, 102083 https://doi.org/10.1016/j.jag.2020.102083.

Bochenek, Z., Shrestha, S., Malek, I., 2013. Hybrid approach for mapping wetland habitats based on application of VHR satellite images. Geoinf. Issues. 5 (1), 21–28. https://doi.org/10.34867/gi.2013.2.

Bond, W.J., Midgley, G.F., 2012. Carbon dioxide and the uneasy interactions of trees and savannah grasses. Phil. Trans. R. Soc. B 367, 601–612. https://doi.org/10.1098/rstb.2011.0182.

Bourgeau-Chavez, L., Endres, S., Battaglia, M., Miller, M.E., Banda, E., Laubach, Z., Higman, P., Chow-Fraser, P., Marcaccio, J., 2015. Development of a bi-national Great Lakes coastal wetland and land use map using three-season PALSAR and Landsat Imagery. Rem. Sens. 7, 8655–8682. https://doi.org/10.3390/rs70708655.

Breiman, L., 2001. Random forests. Mach. Learn. 45, 5–32.

CBD (Secretariat of the Convention on Biological Diversity. (2021). First draft of the Post-2020 global biodiversity framework. https://www.cbd.int/doc/c/abb5/591f/2e46096d3f0330b08ce87a45/wg2020-03-03-en.pdf.

Campoy, J.A., Ruiz, D., Egea, J., 2011. Dormancy in temperate fruit trees in a global warming context: a review. Sci. Hortic. 130 (2), 357–372.

Carle, M.V., Wang, L., Sasser, C.E., 2014. Mapping freshwater marsh species distributions using WorldView-2 high-resolution multispectral satellite imagery. Int. J. Rem. Sens. 35 (13), 4698–4716. https://doi.org/10.1080/01431161.2014.989685.

Crichton, K.A., Anderson, K., Bennie, J.J., Milton, E.J., 2015. Characterizing peatland carbon balance estimates using freely available Landsat ETM+ data. Ecohydrology 8, 493–503. https://onlinelibrary.wiley.com/doi/epdf/10.1002/eco.1519.

Dash, J., Curran, P.J., 2004. The MERIS terrestrial chlorophyll index. Rem. Sens. 25 (23), 5403–5413. https://doi.org/10.1080/0143116042000274015.

Department of Rural Development and Land Reform: National Geo-Information (DRDLR:NGI), 2016. Contours (5-m Interval) and Spot Heights (1:10 000) Related to the Orthophoto Maps provided Digitally. Mowbray, Cape Town, South Africa.

Digital Globe Pty Ltd, 2014. WorldView-3 Data Sheet. https://www.spaceimagingme.com/downloads/sensors/datasheets/DG_WorldView3_DS_2014.pdf. (Accessed 7 October 2022). accessed.

Drovnova, I., Gong, P., Clinton, N.E., Wang, L., Fu, W., Qi, S., Liu, Y., 2012. Landscape analysis of wetland plant functional types: the effects of image segmentation scale, vegetation classes and classification methods. Remote Sens. Environ. 127, 357–369.

Dubeau, P., King, D.J., Unbushe, D.G., Rebelo, L.-M., 2017. Mapping the Dabus wetlands, Ethiopia, using Random Forest classification of Landsat, PALSAR and topographical data. Rem. Sens. 9, 1056. https://doi.org/10.3390/rs9101056.

Environmental Systems Research Institute (ESRI), 1999-2016. ArcGIS Desktop 10.3. ESRI, United States of America, Redlands, CA.

European Space Agency (ESA), 2019a. SeNtinel APplication (SNAP). Platform Version 6.07 accessed during 2018 and 2019). http://step.esa.int.

European Space Agency (ESA), 2019b. Sentinel Online. Retrieved from URL. https://sentinel.esa.int/web/sentinel/missions/sentinel-2/instrument-payload/resolution-and-swath.

Ferreira, M.P., Wagner, F.H., , L.E.O.C., Shimabukuro, Y.E., De Souza Filho, C.R., 2019. Tree species classification in tropical forests using visible to shortwave infrared WorldView-3 images and texture analysis. ISPRS J. Photogrammetry Remote Sens. 149, 119–131.

Ferreira, M.P., Zortea, M., Zanotta, D.C., Shimabukuro, Y.E., De Souza Filho, C.R., 2016. Mapping tree species in tropical seasonal semi-deciduous forests with hyperspectral and multispectral data. Remote Sens. Environ. 179, 66–78.

Fourie, L., Rouget, M., Lötter, M., 2014. Landscape connectivity of the grassland biome in Mpumalanga, South Africa. Austral Ecol. 40, 67–76. https://doi.org/10.1111/aec.12169.

Franke, E., Hall, M.A., Witten, I.A., 2016. The WEKA Workbench. Online Appendix for "Data Mining: Practical Machine Learning Tools and Techniques", Morgan Kaufmann, fourth ed. University of Wakaito, Hamilton, New Zealand.

Freeman, E., Frescino, T., 2009. ModelMap: Modeling and Map Production Using Random Forest and Stochastic Gradient Boosting. United States Department of Agriculture Forest Service. Rocky Mountain Research Station, 507 25th street, Ogden, Utah, United States of America.

Gao, B.-C., 1996. NDWI - a normalized difference water index for remote sensing of vegetation liquid water from space. Remote Sens. Environ. 58, 257–266.

GeoTerraImage (PTY) LTD (GTI), 2015. Technical Report: 2013/2014 South African National Land Cover Dataset Version 5. GeoTerraImage, Pretoria, 53.

Gianinetto, M., Lechi, G., 2004. The development of superspectral approaches for the improvement of land cover classification. IEEE Trans. Geosci. Rem. Sens. 42 (11), 2670–2679.

Gitelson, A.A., Kaufman, Y.J., Merzlyak, M.N., 1996. Use of a green channel in remote sensing of global vegetation from EOS-MODIS. Remote Sens. Environ. 58, 289–298.

Gitelson, A., Merzlyak, M.N., 1994. Spectral reflectance changes associated with autumn senescence of *Aesculus hippocastanum* L. and *Acer platanoides L*. leaves. Spectral features and relation to chlorophyll estimation. J. Plant Physiol. 143, 286–292.

Google Earth Pro (GEP) version 7.3.3.7786, 2022. Die Vlei, Hogsback, at approximate location 32◦ 33’45.06”S; 26◦ 58’10.25”E and eye altitude 4.7 km. Image composite from Maxar Technologies and CNES Airbus images for 8 September 2016. Available from the server kh.google.com and online. http://www.earth. google.com.

Intergovernmental Science-Policy Platform on Biodiversity and Ecosystem Services (IPBES), 2019. In: Díaz, S., Settele, J., Brondízio, E.S., Ngo, H.T., Guèze, M., Agard, J., Arneth, A., Balvanera, P., Brauman, K.A., Butchart, S.H.M., Chan, K.M.A., Garibaldi, L.A., Ichii, K., Liu, J., Subramanian, S.M., Midgley, G.F., Miloslavich, P., Molnár, Z., Obura, D., Pfaff, A., Polasky, S., Purvis, A., Razzaque, J., Reyers, B., Chowdhury, R.R., Shin, Y.J., Visseren-Hamakers, I.J., Willis, K.J., Zayas, C.N. (Eds.), Summary for policymakers of the global assessment report on biodiversity and ecosystem services of the Intergovernmental Science-Policy Platform on Biodiversity and Ecosystem Services. IPBES secretariat, Bonn, Germany, p. 56. https://doi.org/10.5281/zenodo.3553579.

Immitzer, M., Atzberger, C., Koukal, T., 2012. Tree species classification with Random Forest using very high spatial resolution 8-band WorldView-2 satellite data. Rem. Sens. 4, 2661–2693. https://doi.org/10.3390/rs4092661.

Janks, M.R., 2014. Montane Wetlands of the South African Great Escarpment: Plant Communities and Environmental Drivers. MSc thesis. Rhodes University, Grahamstown, South Africa.

Jarman, M.L., 1981. Remote Sensing Applications in Vegetation Mapping, with Special Reference to the Langebaan Area. University of Cape Town, Cape Town, South Africa. South Africa. M.Sc. thesis.

Keith, D.A., Ferrer-Paris, J.R., Nicholson, E., Bishop, M.J., Polidoro, B.A., Ramirez-Llodra, E., Tozer, M.G., Nel, J.L., MacNally, R., Gregr, E.J., Watermeyer, K.E., Essl, F., Faber-Langendoen, D., Franklin, J., Lehmann, C.E.R., Etter, A., Roux, D.J., Stark, J.S., Rowland, J.A., Brummitt, N.A., Fernandez-Arcaya, U.C., Suthers, I. M., Wiser, S.K., Donohue, I., Jackson, L.J.,

Pennington, R.T., Pettorelli, N., Andrade, A., Kontula, T., Lindgaard, A., Tahvanainan, T., Terauds, A., Venter, O., Watson, J.E.M., Chadwick, M.A., Murray, N.J., Moat, J., Pliscoff, P., Zager, I., Kingsford, R.T., 2020. The IUCN Global Ecosystem Typology v1.01: Descriptive Profiles for Biomes and Ecosystem Functional Groups. Available online at: https://iucnrle.org/static/media/uploads/references/research-development/keith_etal_iucnglobalecosystemtypology_v1.01.pdf. (Accessed 25 February 2021). accessed.

Keith, D.A., Ferrer-Paris, J.R., Nicholson, E., Bishop, M.J., Polidoro, B.A., Ramirez-Llodra, E., Tozer, M.G., Nel, J.L., MacNally, R., Gregr, E.J., Watermeyer, K.E., Essl, F., Faber-Langendoen, D., Franklin, J., Lehmann, C.E.R., Etter, A., Roux, D.J., Stark, J.S., Rowland, J.A., Brummitt, N.A., Fernandez-Arcaya, U.C., Suthers, I. M., Wiser, S.K., Donohue, I., Jackson, L.J., Pennington, R.T., Iliffe, T.M., Gerovasileiou, V., Giller, P., Robson, B.J., Pettorelli, N., Andraye, A., Lindgaard, A., Tahvanainen, T., Terauds, A., Chadwick, M.A., Murray, N.J., Moat, J., Pliscoff, P., Zager, I., Kinfsford, R.T., 2022. A function-based typology for Earth's ecosystems. Nature. https://doi.org/10.1038/s41586-022-05318-4.

Knoth, C., Klein, B., Prinz, T., Kleinebecker, T., 2013. Unmanned aerial vehicles as innovative remotesensing platforms for high-resolution infrared imagery to support restoration monitoring in cut-over bogs. Appl. Veg. Sci. 16, 509–517. https://onlinelibrary.wiley.com/doi/epdf/10.1111/avsc.12024.

Linström, A., 2014. Wetland status Quo report: Chrissiesmeer proct. Tevrede Pan Wetland W55A (Wetlands W55A-01-04). In: Lowies, M. (Ed.), SANBI Rehabilitation Plan for the Chrissiesmeer Wetland Project, Mpumalanga: Planning Year 2015/2016. Prepared by Margaret Lowies, Aurecon South Africa (Pty) Ltd. as Part of the Planning Phase for the Working for Wetlands Rehabilitation Programme. Report No. 109664/8810, South African National Biodiversity Institute (SANBI). Pretoria, South Africa.

Linström, A., 2015. Wetland status Quo report: Chrissiesmeer project. Tevrede Pan Wetland W55A (Wetlands W55A - 05 to 07). In: Lowies, M. (Ed.), SANBI Rehabilitation Plan for the Chrissiesmeer Wetland Project, Mpumalanga Province: Planning Year 2015/2016. Prepared by Margaret Lowies, Aurecon South Africa (Pty) Ltd as Part of the Planning Phase for the Working for Wetlands Rehabilitation Programme. Report No. 109664/9589, South African National Biodiversity Institute (SANBI). Pretoria, South Africa.

Liu, X., Liu, H., Qiu, D., Wu, X., Tian, Y., Hao, Q., 2017. An improved estimation of regional fractional Woody/herbaceous cover using combined satellite data and high-Quality training samples. Rem. Sens. 9 (32) https://doi.org/10.3390/rs9010032.

Lück-Vogel, M., Mbolambi, C., Rautenbach, K., Adams, J., Van Niekerk, L., 2016. Vegetation mapping in the St Lucia estuary using very high resolution multispectral imagery and LiDAR. South Afr. J. Bot. 107, 188–199.

McCarthy, T., Cairncross, B., Huizenga, J., Batchelor, A., 2007. Conservation of the Mpumalanga Lakes District. Technical Report. School of Geosciences, University of the Witwatersrand, Johannesburg and Wetland Consulting Services (Pty) Ltd, South Africa.

Mofutsanyana, S.S., 2017. Relationship Among Functional Traits of Wetland Plants and Climatic Variables along an Aridity Gradient across the Highveld, South Africa. M Sc. thesis, University of the Free State (UFS), South Africa. https://scholar.ufs.ac.za/handle/11660/7327. (Accessed 21 December 2021). accessed.

Mofutsanyana, S.S., Collins, N.B., Adelabu, S.A., Chatanga, P., Sieben, E.J.J., 2020. Changes in plant functional composition of wetland vegetation along an aridity gradient on the Highveld plateau of South Africa. Appl. Veg. Sci. 23, 622–634. https://doi.org/10.1111/avsc.12517.

Mucina, L., Rutherford, M.C., 2006. The Vegetation of South Africa, Lesotho and Swaziland. South African National Biodiversity Institute (SANBI) Strelitzia Publication, Pretoria, South Africa.

Mueller-Wilm, U., 2017. Sentinel 2 MPC - Sen2Cor Configuration and User Manual. European Space Agency (ESA), pp. 1–56. Issue 1; Date: 2018-03-22.

Mulhouse, J.M., De Steven, D., Lide, T.F., Sharitz, R.R., 2005. Effect of dominant species on vegetation change in Carolina Bay wetlands following a multi-year drought. J. Torrey Bot. Soc. 132, 411–420.

Naidoo, L., Cho, M.A., Mathieu, R., Asner, G., 2012. Classification of savanna tree species, in the Greater Kruger National Park region, by integrating hyperspectral and LiDAR data in a Random Forest data mining environment. ISPRS J. Photogrammetry Remote Sens. 69, 167–179.

Naidoo, L., Van Deventer, H., Ramoelo, A., Mathieu, R., Nondlazi, B., Gangat, R., 2019. Estimating above ground biomass as an indicator of carbon storage in vegetated wetlands of the grassland biome of South Africa. Int. J. Appl. Earth Obs. Geoinf. 78, 118–129. https://doi.org/10.1016/j.jag.2019.01.021.

Niculescu, S., Boissonnat, J.-B., Lardeux, C., Roberts, D., Hanganu, J., Billey, A., Constantinescu, A., Doroftei, M., 2020. Synergy of high-resolution radar and optical images satellite for identification and mapping of Wetland macrophytes on the Danube Delta. Rem. Sens. 12, 2188. https://doi.org/10.3390/rs12142188.

Olofsson, P., Foody, G.M., Stehman, S.V., Woodcock, C.E., 2013. Making better use of accuracy data in land change studies: estimating accuracy and area and quantifying uncertainty using stratified estimation. Remote Sens. Environ. 129, 122–131.

Olofsson, P., Foody, G.M., Herold, M., Stehman, S.V., Woodcock, C.E., Wulder, M.A., 2014. Good practices for estimating area and assessing accuracy of land change (Review paper). Remote Sens. Environ. 148, 42–57.

Omer, G., Mutanga, O., Abdel-Rahman, E.M., Adam, E., 2015. Performance of support vector machines and Artificial neural network for mapping endangered tree

species using WorldView-2 data in DukuDuku forest, South Africa. IEEE J. Sel. Top. Appl. Earth Obs. Rem. Sens. 99, 1–16.

Pekel, J.-F., Cottam, A., Gorelick, N., Belward, A.S., 2016. High-resolution mapping of global surface water and its long-term changes. Nature 540, 418–422. https://doi.org/10.1038/nature20584. http://www.nature.com/articles/nature20584.pdf.

Pu, R., Landry, S., 2012. A comparative analysis of high spatial resolution IKONOS and WorldView-2 imagery for mapping urban tree species. Remote Sens. Environ. 124, 516–533 (0).

R Core Team, 2009-2021. R: A Language and Environment for Statistical Computing. R Foundation for Statistical Computing, Vienna, Austria. RStudio, 2009-2021. http://www.R-project.org/. Used in the RStudio environment, Version 1.4.1717. http://www.rstudio.com/.

Rajah, P., Odindi, J., Mutanga, O., Kiala, Z., 2019. The utility of sentinel-2 vegetation indices (VIs) and sentinel-1 synthetic Aperture radar (SAR) for invasive alien species detection and mapping. Nat. Conserv. 35, 41–61. https://doi.org/10.3897/natureconservation.35.29588.

Rapinel, S., Mony, C., Lecoq, L., Clément, B., Thomas, A., Hubert-Moy, L., 2019. Evaluation of Sentinel-2 time-series for mapping floodplain grassland plant communities. Remote Sens. Environ. 223, 115–129. https://doi.org/10.1016/j.rse.2019.01.018.

Richardson, A.D., Keenan, T.F., Migliavacca, M., Ryu, Y., Sonnentag, O., Toomey, M., 2013. Climate change, phenology, and phenological control of vegetation feedbacks to the climate system. Agric. For. Meteorol. 169, 156–173.

Richter, R., Schläpfer, D., 2015. Atmospheric/Topographic Correction for Satellite Imagery - ATCOR-2/3 User Guide. June 2015, Version 9.0.0. http://www.rese.(Accessed 14 February 2019). accessed.

Rouse, J., Hass, R., Schell, J., Deering, D., 1973. Monitoring vegetation systems in the Great plains with ERTS. In: Third ERTS Symposium, NASA, SP-351 I, pp. 309–317.

Sardans, J., Peñuelas, J., 2012. The role of plants in the effects of global change on nutrient availability and stoichiometry in the plant-soil system. Plant Physiol. 160, 1741–1761.

Schmidt, K.S., Skidmore, A.K., 2003. Spectral discrimination of vegetation types in a coastal wetland. Remote Sens. Environ. 85 (1), 92–108. https://doi.org/10.1016/S0034-4257(02)00196-7.

Sieben, E.J.J., Mtshali, H., Janks, M., 2014. National Wetland Vegetation Database: classification and analysis of wetland vegetation types for conservation planning and monitoring. In: Water Research Commission (WRC). WRC, Pretoria, South Africa, p. 241. Report No. K5/1980.

Skowno, A., Raimondo, D., Powrie, L., Hoffman, M.T., Van der Merwe, S., Hlahane, K., Fizzoti, B., Varaiwa, T., 2019. Chapter 3: Pressures and Threats. South African National Biodiversity Assessment 2018: Technical Report. In: Terrestrial Environment, vol. 1. South African National Biodiversity Institute (SANBI), Pretoria, South Africa. Report Number: SANBI/NAT/NBA2018/2019/Volx/A.

Stevens, N., Erasmus, B.F.N., Archibald, S., Bond, W.J., 2016. Woody encroachment over 70 years in South African savannahs: overgrazing, global change or extinction aftershock? Philos. Trans. R. Soc. Lond. B Biol. Sci. 371 (1703), 20150437 https://doi.org/10.1098/rstb.2015.0437.

Story, M., Congalton, R., 1986. Accuracy assessment: a user's perspective. Photogramm. Eng. Rem. Sens. 52, 397–399.

Tucker, C.J., 1979. Red and photographic infrared linear combinations for monitoring vegetation. Remote Sens. Environ. 8 (2), 127–150.

Turak, E., Harrison, I., Dudgeon, D., Abell, R., Bush, A., Darwall, W., Finlayson, C.M., Ferrier, S., Freyhof, J., Hermoso, V., Juffe-Bignoli, D., Linke, S., Nel, J., Patricio, H.C., Pittock, J., Raghaven, R., Revenga, C., Simaika, J.P., De Wever, A., 2017. Essential Biodiversity Variables for measuring change in global freshwater biodiversity. Biol. Conserv. 213, 272–279. https://doi.org/10.1016/j.biocon.2016.09.005.

United Nations (UN), 2017. Integrated Monitoring Guide for SDG 6: Step-by-step Monitoring Methodology for Indicator 6.6.1 on Water-Related Ecosystems. Version 20 January 2017. http://www.unwater.org/app/uploads/2017/05/Step-by-step-methodology-6-6-1_Revision-2017-01-20_Final-1.pdf.

Van Deventer, H., 2021. Monitoring changes in South Africa's surface water extent for reporting Sustainable Development Goal sub-indicator 6.6.1. a. S. Afr. J. Sci. 117 (5/6) https://doi.org/10.17159/sajs.2021/8806. Art. #8806.

Van Deventer, H., Cho, M.A., Mutanga, O., 2017. Improving the classification of six evergreen subtropical tree species with multi-season data from leaf spectra simulated to WorldView-2 and RapidEye. Int. J. Rem. Sens. 38 (17), 4804–4830. https://doi.org/10.1080/01431161.2017.1320445.

Van Deventer, H., Cho, M.A., Mutanga, O., 2019. Multi-season RapidEye imagery improves the classification of wetland and dryland communities in a subtropical coastal region. ISPRS J. Photogrammetry Remote Sens. 157, 171–187. https://doi.org/10.1016/j.isprsjprs.2019.09.007.

Van Deventer, H., Linström, A., Durand, J.F., Naidoo, L., Cho, M.A., 2022. Deriving the maximum extent and hydroperiod of open water from Sentinel-2 imagery for global sustainability and biodiversity reporting for wetlands. WaterSA 48 (1).

Van Deventer, H., Naidoo, L., Cho, M.A., Job, N.M., Linström, A., Sieben, E., Snaddon, K., Gangat, R., 2020a. Establishing Remote Sensing Toolkits for Monitoring Freshwater Ecosystems under Global Change. Water Research Commission Report No. 2545/1/19. Available online at: http://wrcwebsite.azurewebsites.net/mdocs-posts/establishing-remote-sensing-toolkits-for-monitoring-freshwater-ecosystems-under-global-change/.

Van Deventer, H., Nel, Jeanne L., Mbona, N., Job, N., Ewart-Smith, J., Snaddon, K., Maherry, A., 2016. Desktop classification of inland wetlands for systematic conservation planning in data-scarce countries: mapping wetland ecosystem types, disturbance indices and threatened species associations at country-wide scale using GIS. Aquat. Conserv. Mar. Freshw. Ecosyst. 26, 57–75. https://doi.org/10.1002/aqc.2605.

Van Deventer, H., Van Niekerk, L., Adams, J., Dinala, M.K., Gangat, R., Lamberth, S.J., Lötter, M., Mbona, N., MacKay, F., Nel, J.L., Ramjukadh, C.-L., Skowno, A., Weerts, S.P., 2020b. National Wetland Map 5 - an improved spatial extent and representation of inland aquatic and estuarine ecosystems in South Africa. WaterSA 46 (1), 66–79. https://doi.org/10.17159/wsa/2020.v46.i1.7887.

Waywell, T., 2009. The effect of various map projections on surface area. PositionIT July 49–55.

World Resources Institute (WRI), 2000. Compiled by. In: White, R.P., Murray, S., Rohweder, M. (Eds.), Pilot analysis of Global Ecosystems: Grassland Ecosystems. http://pdf.wri.org/page_grasslands.pdf. (Accessed 21 December 2021). accessed.

Zoungrana, B.J.B., Conrad, C., Amekudzi, L.K., Thiel, M., Da, E.D., Forkuor, G., Löw, F., 2015. Multi-temporal Landsat images and ancillary data for land use/cover change (LULCC) detection in the Southwest of Burkina Faso, West Africa. Rem. Sens. 7, 12076–12102. https://doi.org/10.3390/rs70912076.